Monodispersed Fullerene Derivatives Introduced into the Channels of Mesoporous Silica via Chemical Bond Interactions

Huixia Wu,[1,2] Yanghui Lin,*[1] Jiawei Tang,[1] Dong Gao,[1] Ruifang Cai,[1] and Dongyuan Zhao*[1]

[1]Department of Chemistry, Fudan University, Shanghai 200433, P. R. China

[2]Department of Chemistry, Shanghai Normal University, Shanghai 200234, P. R. China

Received September 7, 2006; E-mail: lyanghui@fudan.edu.cn

A specific fullerene derivative, $C_{60}(CHCOOH)_2$, was introduced into the matrix network of well-ordered hexagonal mesoporous silica (SBA-15) via a chemical bond interaction. The methods included aminosilylation of the surface silanols within SBA-15 channels by 3-aminopropyl(trimethoxy)silane (APTS) and a subsequent amide reaction between amino groups of APTS/SBA-15 and carboxylic acids of $C_{60}(CHCOOH)_2$. The final material $C_{60}(CHCOOH)_2$/APTS/SBA-15 was confirmed by XRD, TEM, and BET techniques, FT-IR and UV–vis spectra. The [60]fullerene carboxylic derivative molecules were uniformly distributed in the channels of SBA-15, while pure [60]fullerene molecules remained as clusters or larger aggregate states.

Since the discovery of C_{60} and the improvement of its preparative methods, fullerenes have attracted much attention for a wide range of potential applications in optical, electronic, magnetic, physiological, and even medical usage.[1–5] Recently, “single molecular chemistry” taking place in nanostructure environments has caused much interest in the chemical community. Reactions in which molecules are spatially restrained could lead to a new fundamental understanding about the use of the local environment to control chemical reactions.[6,7] The incorporation of fullerenes and their derivatives in inorganic host matrixes to fabricate organic–inorganic nanocomposites is very important and has promising applications especially in material usage.[8] Up to now, fullerenes are have usually been introduced into the matrix network by a postpreparation approach, no attempts to graft fullerene derivatives to the backbone have been reported to our knowledge.[9] Several difficulties have challenged scientists in developing this type of nanocomposite materials,[9,10] such as the insolubility of fullerene in polar organic solvents and the difficulty in controlling the aggregation state of fullerenes and their derivatives. The properties of the material appear to be affected by the state of the fullerenes. It has been shown that when C_{60} molecules aggregate, the formation of the triplet state considerably decreases, thus reducing the optical limiting capability of such aggregate molecules.[11] Therefore, if fullerenes are incorporated as isolated molecules, rather than clusters or larger aggregates, the properties should improve.

In this work, isolated fullerene carboxylic derivative molecules were incorporated into the channels of mesoporous silica (SBA-15) via chemical bonding with the matrix network. The solubility of fullerene in polar organic solvents was improved by functionalizing the fullerene with a polar carbonyl functional group. At the same time, the fullerene derivative molecules were prevented from aggregating by their direct chemical bond with the matrix network in mesoporous silica (SBA-15). The resulting surface modification of SBA-15 should maintain or improve the optical properties of the grafted fullerene derivative.[11]

Experimental

Characterization Instruments. X-ray diffractometer (XRD) patterns were recorded on a Bruker D8 Advanced X-ray diffractometer using Cu Kα radiation. FT-IR spectra were measured on Nicolet FT-IR-50-X. Diffuse reflectance UV–vis spectra were recorded on a JASCO Corp. V-550. Thermal gravimetric analyses (TGA) were performed on a Perkin-Elemer Pyris 1 DTA-TGA instrument under nitrogen with a heating rate of $10\,^\circ\mathrm{C\,min^{-1}}$. Transmission electron microscopy (TEM) experiments were conducted on a JEOL2011 microscope operated at 200 kV. Photoluminescence excitation data were obtained on a Cary Eclipse fluorescence spectrometer. The Nitrogen adsorption–desorption isotherms were measured using a Micromeritics ASAP 2000 system, the samples were degassed at 473 K overnight on a vacuum line.

Synthesis of Materials. The synthetic route of $C_{60}(CHCOOH)_2$/APTS/SBA-15 is described in Scheme 1.

$C_{60}{}^{2-}$ anion was prepared in THF solution according to the previously described method.[12] To the above $C_{60}{}^{2-}$ anion solution in THF (20 mL, 0.50 mmol) was added dibromo-reagent of fumarate (80 mg, 0.50 mmol) while stirring, and the mixture was refluxed at 333 K. After reacting for 4 h, an air-stable brown powder precipitated from the solution, was centrifuged and washed twice with THF. Solvent residues were removed by freeze drying under vacuum for several hours. Dilute hydrochloric acid (15 mL, 6 M) was added to the above solid. After acidification for 6 h, the mixture was centrifuged and the solid was washed twice with water. Finally, the product was dried at 333–343 K to remove the remaining water under high vacuum for 24 h, the obtained $C_{60}(CHCOOH)_2$ was confirmed by FT-IR, FD-MS, ^{1}H NMR, and UV–vis spectra.[13]

SBA-15[14] was synthesized under acidic conditions using tetraethyl orthosilicate (TEOS 98%, Aldrich) as a silicon source and the tri-block copolymer poly(ethylene oxide)–poly(propylene oxide)–poly(ethylene oxide) ($EO_{20}PO_{70}EO_{20}$, Aldrich) as a tem-

Published on the web May 14, 2007; doi:10.1246/bcsj.80.994

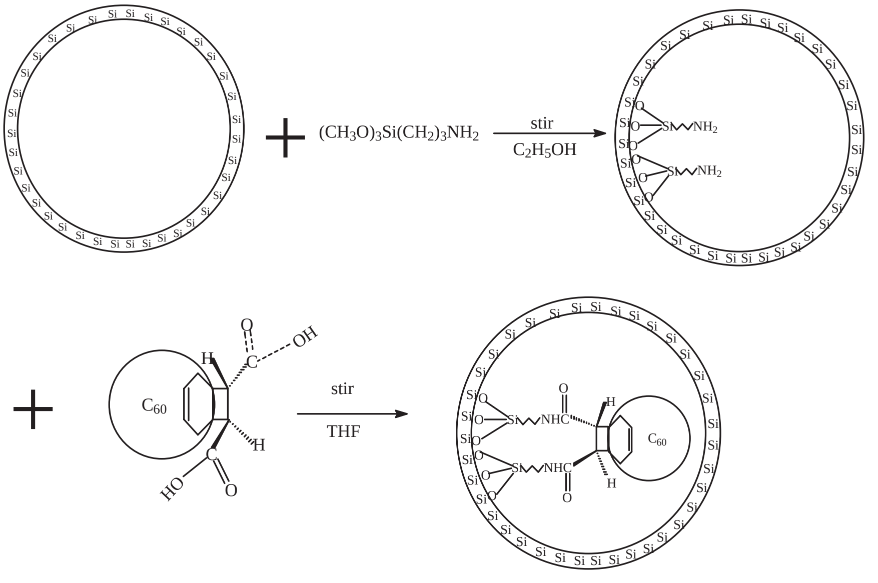

Scheme 1.

plate. A solution with the mass ratio of $EO_{20}PO_{70}EO_{20}$:2MHCl:TEOS:H_2O = 2:80:4.25:15 was prepared, stirred for 4 h at 313 K, and then heated at 373 K for 24 h. The solid product was filtered and calcinated at 823 K for 5 h. The SBA-15 obtained has a mean pore diameter of 8.14 nm, a pore volume of 1.21 $cm^3\,g^{-1}$, and a BET surface area of 577 $m^2\,g^{-1}$ was determined by N_2 adsorption–desorption measurement at 77 K. Before the aminosilylation reaction, the SBA-15 sample was dried at room temperature for 8 h under vacuum.

Aminosilylation reaction of SBA-15 was performed according to the literature method with minor modification.[15] In a typical preparation, SBA-15 (1 g) was refluxed for 12 h in ethanol solution (25 mL) containing 1 wt % 3-aminopropyl(trimethoxy)silane (APTS). The resulting material, APTS/SBA-15, was collected by filtration, washed twice with ethanol, and dried at room temperature for 24 h under vacuum to remove the remaining solvent. To directly bond the fullerene dicarboxylic derivative on the matrix network in mesoporous silica (SBA-15), APTS/SBA-15 (0.5 g) was stirred and refluxed in a THF solution (20 mL) containing of fullerene derivative $\{C_{60}(CHCOOH)_2\}$ (10 mg) at 70 °C for 3 h. After the stirring was stopped for 20 min, the color of the solution turned from brown to colorless, and the precipitate of APTS/SBA-15 changed color from white to light brown. The resulting solid, $C_{60}(CHCOOH)_2$/APTS/SBA-15, was collected by filtration, and washed twice with THF to remove the unanchored $C_{60}(CHCOOH)_2$. Finally, the remaining solvent was removed from product under vacuum.

Fullerene samples C_{60}/APTS/SBA-15, $C_{60}(CHCOOH)_2$/APTS and C_{60}/APTS were prepared for comparison. APTS/SBA-15 (0.5 g) was stirred and refluxed in a toluene solution (20 mL) containing fullerene C_{60} (10 mg) at 120 °C for 3 h. The resulting solid, C_{60}/APTS/SBA-15, was collected by filtration and washed twice with toluene. Finally, the remaining solvent was removed under vacuum.

APTS are dropped into THF solution of $C_{60}(CHCOOH)_2$ and toluene solution of C_{60}, respectively, with a molar ratio of 2:1. After stirring and refluxing for 2 h, the solvent was removed under vacuum. The obtained solids, $C_{60}(CHCOOH)_2$/APTS or C_{60}/APTS, were washed twice with hexane, and dried at room temperature for 24 h under vacuum.

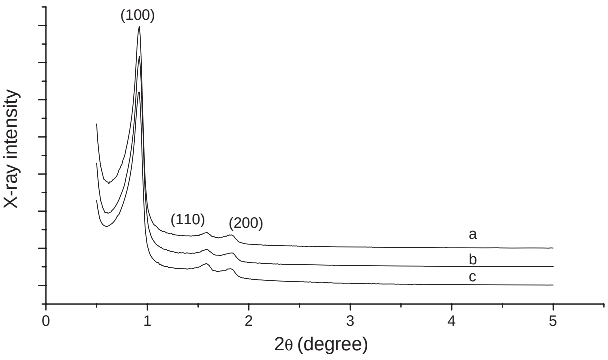

Fig. 1. XRD patterns of (a) $C_{60}(CHCOOH)_2$/APTS/SBA-15, (b) APTS/SBA-15, and (c) SBA-15.

Results and Discussion

In this work, we report that fullerene derivative $C_{60}(CHCOOH)_2$ could be immobilized inside the channels of mesoporous silica SBA-15 and bonded with amino groups of the matrix network in mesoporous silica (SBA-15) after the SBA-15 was aminosilylated by using 3-aminopropyl(trimethoxy)silane to form APTS/SBA-15. It was obvious that $C_{60}(CHCOOH)_2$ anchored to the basic amine groups of APTS/SBA-15 through acid–base neutralization.

Figure 1 shows the XRD patterns of three solid samples SBA-15, APTS/SBA-15, and $C_{60}(CHCOOH)_2$/APTS/SBA-15 in the 2θ range of 0.6–5°.

All samples exhibited three peaks that were indexed as the characteristic (100), (110), and (200) reflections of hexagonal mesoporous SBA-15, indicating that these samples consisted of well-ordered packed channels.[16] Thus, the primary structure of SBA-15 was maintained during aminosilylation of SBA-15 and chemical bonding of $C_{60}(CHCOOH)_2$ with APTS/SBA-15. Meanwhile, the intensity of the three reflections of APTS/SBA-15 and $C_{60}(CHCOOH)_2$/APTS/SBA-15 were nearly the same as those of pure SBA-15. The chemical bonding between $C_{60}(CHCOOH)_2$ and APTS/SBA-15 may prevent the aggregation of fullerene derivative $C_{60}(CHCOOH)_2$, thus keeping the SBA-15 channels unblocked and making the fullerene derivative exist predominantly in monomeric form. This results could be observed via diffuse reflectance UV–vis spectra (discussed later).

The nitrogen adsorption isotherms (Fig. 2) of $C_{60}(CHCOOH)_2$/APTS/SBA-15, APTS/SBA-15, and SBA-15 showed type *I–V* plots with type H1 hysteresis loops for a typical mesoporous material with 1-D cylindrical channels.[17] The pore sizes of calcinated SBA-15, APTS/SBA-15, $C_{60}(CHCOOH)_2$/APTS/SBA-15, and C_{60}/APTS/SBA-15 were 8.14, 7.34, 7.14, and 7.06 nm, respectively, which were calculated from the adsorption branch by using the Barrett–Joyner–Halenda model. Both the BET surface areas and pore volumes of $C_{60}(CHCOOH)_2$/APTS/SBA-15 and C_{60}/APTS/SBA-15 were smaller than those of APTS/SBA-15. The amount of fullerene loaded on the mesoporous silica was determined by TGA of pristine mesoporous silica APTS/SBA-15 and the loaded samples $C_{60}(CHCOOH)_2$/APTS/SBA-15. The experimental results showed the amount of fullerenes loaded on the mesoporous silica was above 80 wt % of the amount of added fullerene derivative. It means that the amount of fullerene C_{60} loaded on the mesoporous silica was about 1.6 wt %. These aspects indirectly proved that fullerene derivative molecules entered into channels of SBA-15.

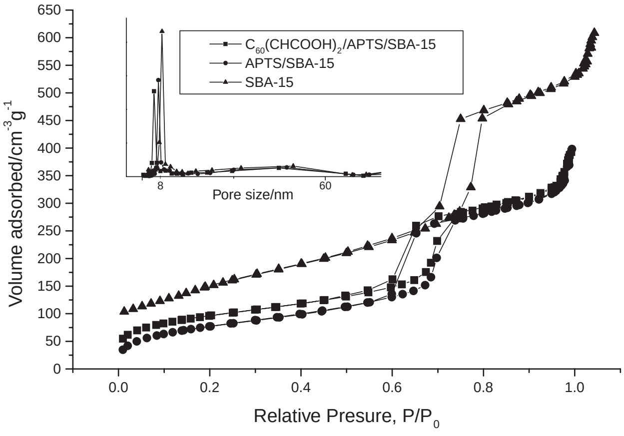

Fig. 2. Nitrogen adsorption–desorption isotherm plots and pore-size distribution curves (inset) of SBA-15 and its functioned materials. The isotherms were measured using a Micromeritics ASAP 2000 system. The samples were degassed at 473 K overnight on a vacuum line.

From TEM images, we observed that the morphologies of $C_{60}(CHCOOH)_2$/APTS/SBA-15, C_{60}/APTS/SBA-15, and SBA-15 were almost similar, which confirmed that fullerene and fullerene derivative did not destroy the outward appearance of SBA-15 channels.

In order to further prove the chemical bonding of $C_{60}(CHCOOH)_2$ with APTS/SBA-15, we measured the FT-IR spectra of three solid samples, that is, SBA-15, APTS/SBA-15, and $C_{60}(CHCOOH)_2$/APTS/SBA-15. In Fig. 3 curve a, a peak at 1652 cm^{-1} belonging to secondary amides –CONH–, which was formed via chemical reaction between amino of APTS/SBA-15 and carboxylic acids of $C_{60}(CHCOOH)_2$, was observed. In addition, we observed a weak N–H bending vibration at 1550 cm^{-1}; its intensity was slightly weaker than that of curve b, which was attributed to the conversion of primary amine to secondary amine. Other IR peaks were observed at 528, 572, and 1428 cm^{-1}, which were consistent with the characteristic peaks of fullerene,[2] and suggested that [60]fullerene molecules maintained their structure. Compared with the IR spectra of $C_{60}(CHCOOH)_2$,[13] The peak at 1708 cm^{-1} was absent, indicating that the –COO$^-$ bond becomes –CONH– in resulting $C_{60}(CHCOOH)_2$/APTS/SBA-15. In the amino-modified SBA-15 sample (curve b), the presence of APTS functional group on the matrix network was verified by the presence of the N–H (primary amine) bending vibration at 1550 cm^{-1}.

Comparing the IR spectra of $C_{60}(CHCOOH)_2$/APTS with those of C_{60}/APTS (Fig. 4), the peak at 1647 cm^{-1} corresponded to a secondary amides (–CONH–), which was formed via chemical reaction between amino of APTS and carboxylic acids of $C_{60}(CHCOOH)_2$, but was shifted 5 cm^{-1}. The peak at 1708 cm^{-1}, which corresponds carboxylic groups was also absent. C_{60} and APTS/C_{60} had almost the same IR spectra, suggesting that APTS cannot chemically react with C_{60} under such conditions. In other words, different conditions must

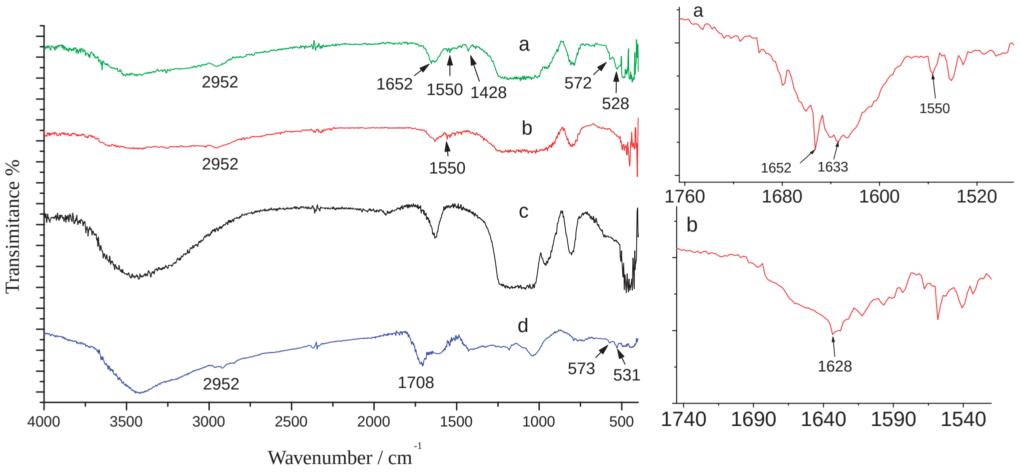

Fig. 3. IR spectra of (a) $C_{60}(CHCOOH)_2$/APTS/SBA-15, (b) APTS/SBA-15, (c) SBA-15, and (d) $C_{60}(CHCOOH)_2$. Water in the samples was removed by freezed drying at 373 K under high vacuum for 24 h.

be found for the chemical reaction between C_{60} and APTS/SBA-15.

The diffuse reflectance UV–vis spectrum of [60]fullerene is known to be sensitive to environmental effects (solvent and aggregation), and can be used to determine the aggregation state. Figure 5 shows the UV–vis spectra of four solid samples SBA-15, APTS/SBA-15, $C_{60}(CHCOOH)_2$/APTS/SBA-15, and the mixture of APTS/SBA-15 and $C_{60}(CHCOOH)_2$.

From Fig. 5 curve a, it was confirmed that the [60]fullerene derivative existed in the SBA-15 channels predominantly in monomeric form, which has a characteristic sharp peak at 396 nm.[18] Meanwhile, we did not observe any band at 450 nm,[19] which is assigned to the formation of aggregates. The aminosilane absorption band at 300 nm[20] was observed as shown in Fig. 5 curve a and b. In Fig. 5 curve a, the long tail band extending to 700 nm[21] was consistent with the saturation due to the double bonds of [60]fullerene, resulting from the reaction of $C_{60}{}^{2-}$ with dibromo-reagent of fumarate. In addition, Fig. 5 curve a had other peaks in the range of 240–340 nm. In a word, curve a is very different from curves b, c, and d. In order to measure the effect of [60]fullerene derivative content on UV–vis spectrum, Figure 6 shows UV–vis spectra of $C_{60}(CHCOOH)_2$/APTS/SBA-15 samples having (a) 2 wt % and (b) 4 wt % [60]fullerene derivative content. Curve b was almost similar to curve a, only the intensity of the former was stronger than that of the latter, thus suggesting that [60]fullerene derivative in SBA-15 channels existed predominantly in monomeric form.

However, for sample C_{60}/APTS/SBA-15, a peak at 449 nm was observed in Fig. 7b, and the intensity of three peaks (100), (110), and (200) were weak, as seen in Fig. 8a. For sample $C_{60}(CHCOOH)_2$/APTS/SBA-15, a peak at 449 nm was not abserved in Fig. 7a, and the intensity of three peaks (100), (110), and (200), were stronger in Fig. 8b. Because the loaded substance cannot be dispersed in the pores of the mesoporous materials uniformly, it will make the structure of the materials become less ordered than the blank ordinary SBA-15. So, the less ordered materials will show broader peaks in the XRD patterns.

Therefore, we believe that the mono-dispersion of fullerene

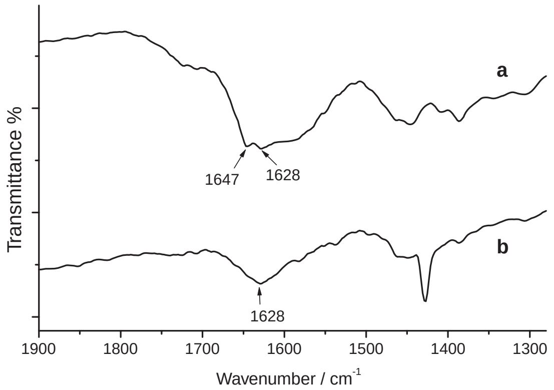

Fig. 4. IR spectra of (a) $C_{60}(CHCOOH)_2$/APTS and (b) C_{60}/APTS. Water in the samples were removed by freezed drying at 373 K under high vacuum for 24 h.

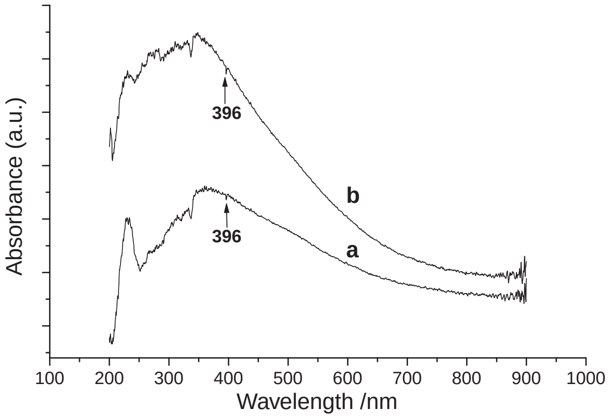

Fig. 6. Diffuse reflectance UV–vis spectra of (a) 2 wt % low and (b) 4 wt % high C_{60} derivative content of $C_{60}(CHCOOH)_2$/APTS/SBA-15.

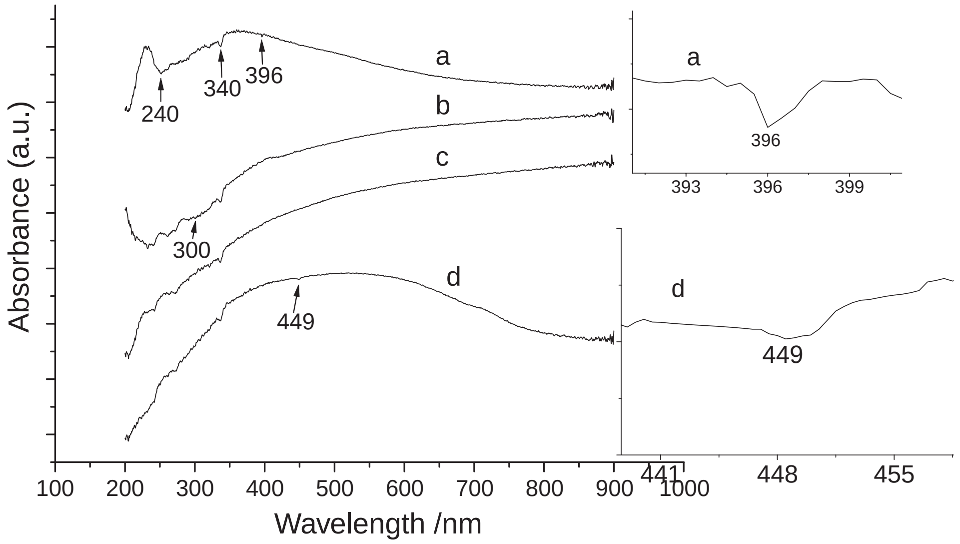

Fig. 5. Diffuse reflectance UV–vis spectra of (a) $C_{60}(CHCOOH)_2$/APTS/SBA-15, (b) APTS/SBA-15, (c) SBA-15, and (d) the mixture of APTS/SBA-15 and $C_{60}(CHCOOH)_2$.

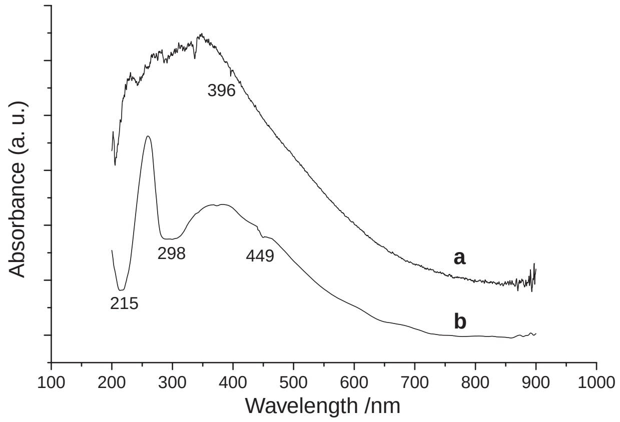

Fig. 7. Diffuse reflectance UV–vis spectra of (a) C_{60}(CH-COOH)$_2$/APTS/SBA-15 and (b) C_{60}/APTS/SBA-15.

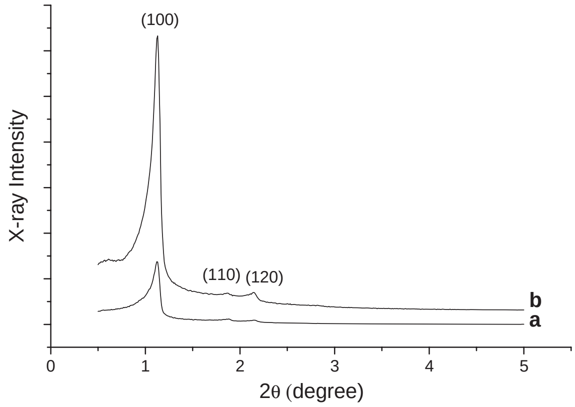

Fig. 8. XRD patterns of (a) C_{60}/APTS/SBA-15 and (b) SBA-15.

derivatives in the mesoporous materials via chemical bond may effectively tune the physical properties of the obtained materials, like surface properties and pore sizes of material channels, which enable these materials to enjoy wide potential applications in matter isolation.

The luminescence of pure [60]fullerene is weak, and [60]fullerene derivatives may exhibit enhanced luminescence.[22] In mesoporous materials, surface properties of nanostructure materials, chemical bonding interaction of [60]fullerene derivatives with mesoporous materials and stored time in air affect luminescence properties.[23,24] We have synthesized some special fullerene derivatives, and we are currently studying their photoluminescence properties. These properties may make them have potential applications in optical and electronic usage.

Conclusion

C_{60}(CHCOOH)$_2$, was chemically grafted to the backbone of mesoporous silica SBA-15. The channels of SBA-15 was aminiosilylated by APTS and subsequently reacted with C_{60}(CHCOOH)$_2$ via acid–base neutralization. Fullerene derivative molecules were monodispersed in channels of SBA-15. The use of mesoporous molecular sieve SBA-15 reported here is a novel method for mono-dispersion of fullerene derivatives, which may make possible to tune in the physical properties of the obtained materials, like surface properties and pore sizes of material channels.

This work was supported by the Shanghai Nature Science Foundation of China (Project No. 04ZR14016) and the National Nature Science Foundation of China (Project No. 20271013).

References

1 H. Shinohara, *Rep. Prog. Phys.* **2000**, *63*, 843.
2 Y. H. Lin, R. F. Cai, Y. Chen, Z.-E. Huang, Y. H. Zhou, G. H. Ma, *J. Mater. Sci. Lett.* **1999**, *18*, 1383.
3 B. O. Skadtchenko, M. Trudeau, R. W. Schurko, M. J. Willans, D. Antonelli, *Adv. Funct. Mater.* **2003**, *13*, 671.
4 L. Y. Ostrovskaya, V. M. Perevertailo, L. A. Matveeva, P. Milani, V. G. Ralchenko, E. M. Shpilevsky, *Powder Metall. Met. Ceram.* **2003**, *42*, 1.
5 D. Gust, T. A. Moore, A. L. Moore, *Acc. Chem. Res.* **2001**, *34*, 40.
6 S. S. Deng, X. L. Wu, Z. Y. Zhang, Y. F. Mei, H. Chen, *Phys. Lett. A* **2002**, *299*, 299.
7 J. Tachibana, M. Chiba, M. Ichikawa, T. Imamura, Y. Sasaki, *Supramol. Sci.* **1998**, *5*, 281.
8 G. Gu, W. P. Ding, Y. W. Du, H. Huang, S. Yang, *Appl. Phys. Lett.* **1997**, *70*, 2619.
9 P. Innocenzi, G. Brusatin, *Chem. Mater.* **2001**, *13*, 3126.
10 S. Subbiah, R. Mokaya, *Chem. Commun.* **2003**, 92.
11 J. M. Janot, E. Bienvenüe, P. Seta, R. V. Bensasson, A. C. Tomé, R. F. Enes, J. A. S. Cavaleiro, S. Leach, X. Camps, A. Hirsch, *J. Chem. Soc., Perkin Trans. 2* **2000**, 301.
12 J. Chen, R.-F. Cai, Z.-E. Huang, H.-M. Wu, S.-K. Jiang, Q.-F. Shao, *J. Chem. Soc., Chem. Commun.* **1995**, 1553.
13 Y. H. Lin, R. F. Cai. *Acta Chim. Sin.* **2005**, *63*, 774.
14 D. Y. Zhao, J. L. Feng, Q. S. Huo, N. Melosh, G. H. Fredrickson, B. F. Chmelka, G. D. Stucky, *Science* **1998**, *279*, 548.
15 W. Kaleta, K. Nowińska, *Chem. Commun.* **2001**, 535.
16 K. K. Zhu, H. Y. He, S. H. Xie, X. Zhang, W. Z. Zhou, S. L. Jin, B. Yue, *Chem. Phys. Lett.* **2003**, *377*, 317.
17 M. J. Yuan, J. W. Tang, C. Z. Yu, Y. H. Chen, B. Tu, D. Y. Zhao, *Chem. Lett.* **2003**, *32*, 660.
18 S. K. Lin, L. L. Shiu, K. M. Chien, T. Y. Luh, T. I. Lin, *J. Phys. Chem.* **1995**, *99*, 105.
19 J. Eastoe, E. R. Crooks, A. Beeby, R. K. Heenan, *Chem. Phys. Lett.* **1995**, *245*, 571.
20 J. Evans, A. B. Zaki, M. Y. Ei-Sheikh, S. A. Ei-Safty, *J. Phys. Chem. B* **2000**, *104*, 10271.
21 I. Lamparth, A. Hirsh, *J. Chem. Soc., Chem. Commun.* **1994**, 1727.
22 A. Mrzel, B. Podobnik, A. Hassanien, D. Mihailovic, M. Ozawa, *Synth. Met.* **1999**, *103*, 2437.
23 B. Hamilton, J. S. Rimmer, M. Anderson, D. Leigh, *Adv. Mater.* **1993**, *5*, 583.
24 M. W. Anderson, J. Shi, D. A. Leigh, A. E. Moody, F. A. Wade, B. Hamilton, S. W. Carr, *J. Chem. Soc., Chem. Commun.* **1993**, 533.